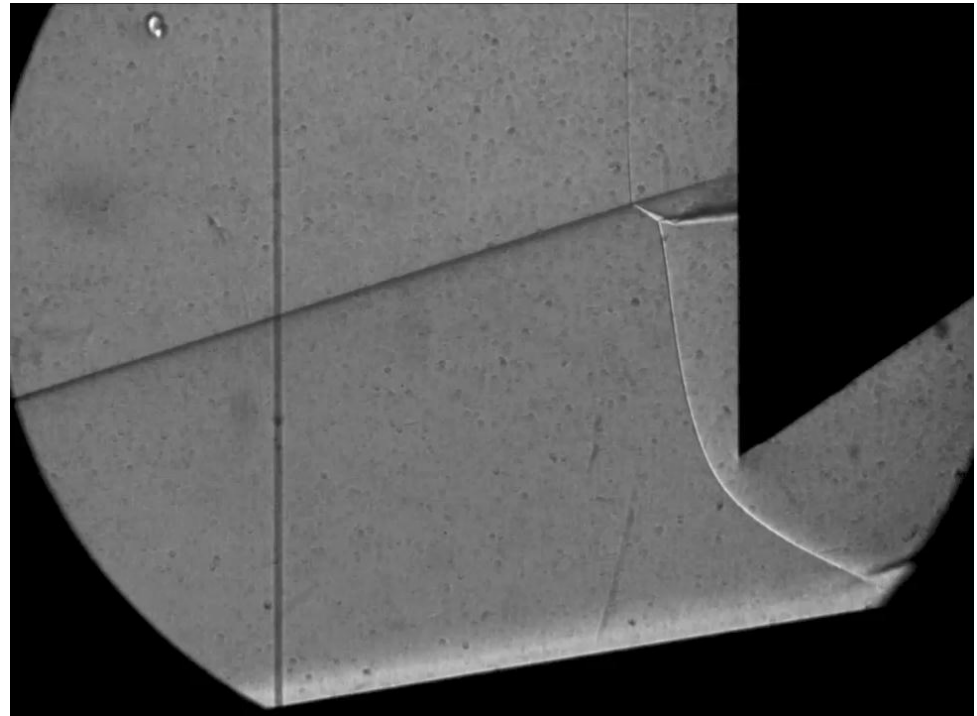
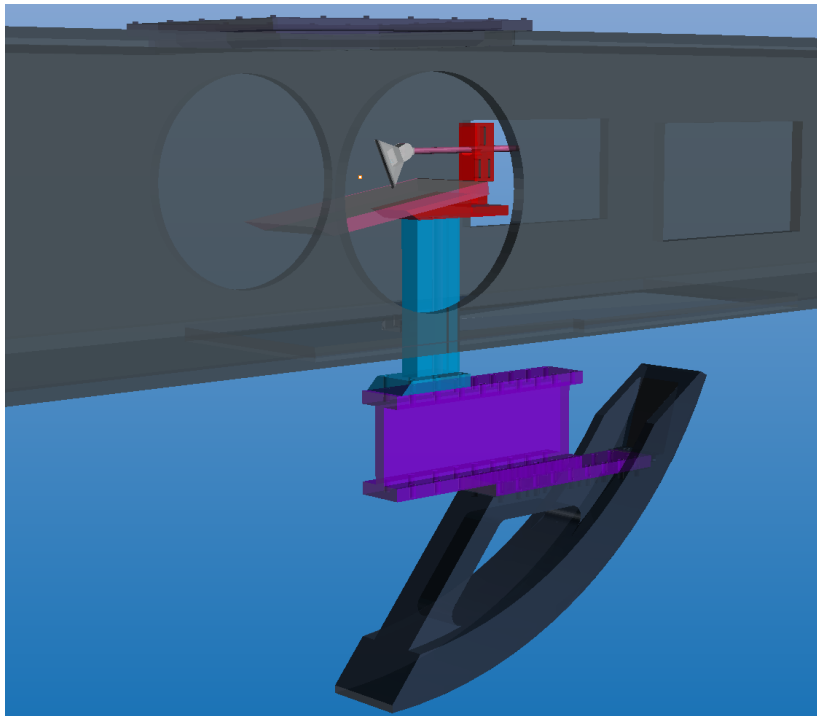




Thermographic Phosphor Measurements of Shock-Shock Interactions on a Swept Cylinder

Michelle Jones, Scott Berry
NASA Langley Research Center



Thermal & Fluids Analysis Workshop (TFAWS 2013)
July 29-August 2, 2013, Kennedy Space Center (KSC), FL



Presentation Outline



Topic	Slides
• Introduction	3
• Historical Perspective	4, 5
• Test Set-up	6-11
• Test Matrix	12
• Results	
– Zoom Schlieren	13
– Oil Flow	14
– Heat Transfer	15-26
• Conclusions	27



The main purpose of this study is to experimentally investigate shock-shock interactions that can affect the surface heating of supersonic and hypersonic flight vehicles

Goals

- Characterize shock-shock interaction patterns and heating with increased resolution
- Analyze the heat transfer using one-dimensional and multi-dimensional techniques

Study Impact

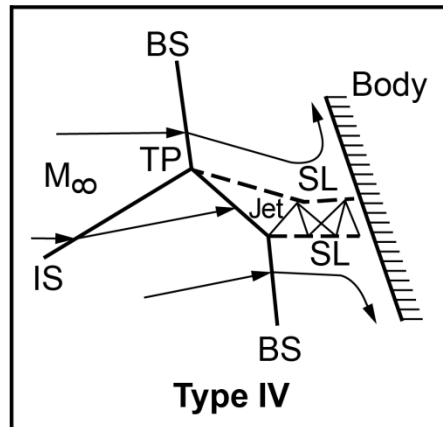
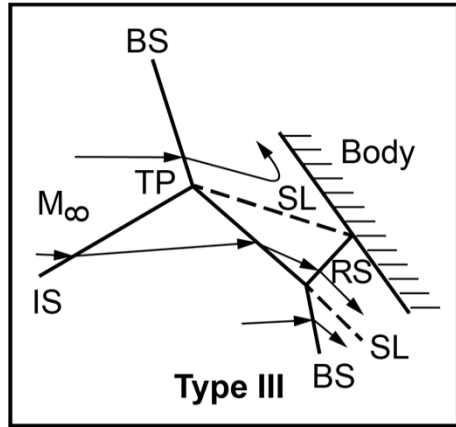
- First published results investigating peak heating augmentation due to shock-shock interactions with global imaging techniques and multi-dimensional thermal analyses
- Contributes to the knowledge of 3D hypersonic shock-on-strut interactions using high-speed zoom schlieren and oil-flow techniques



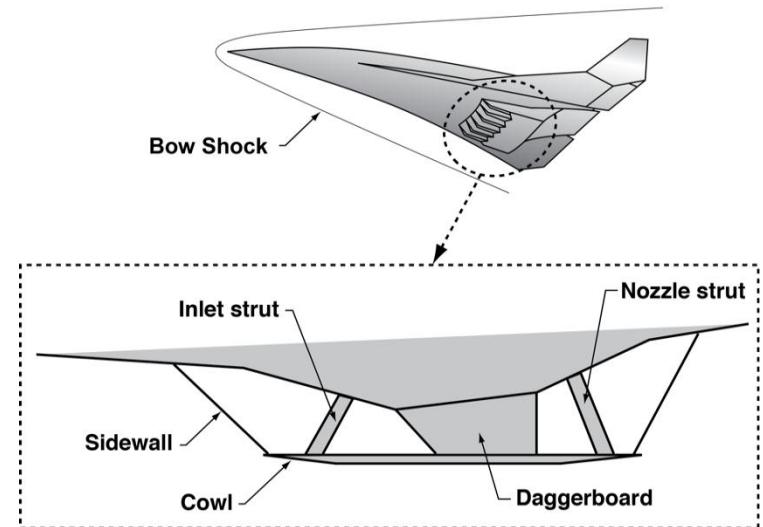
Historical Perspective



Type III and IV Shock-Shock Interactions (Barry Edney, ARI of Sweden, 1968)



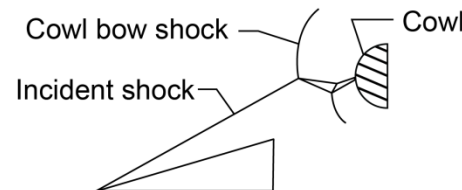
Shock Interaction on Hypersonic Flight Vehicles



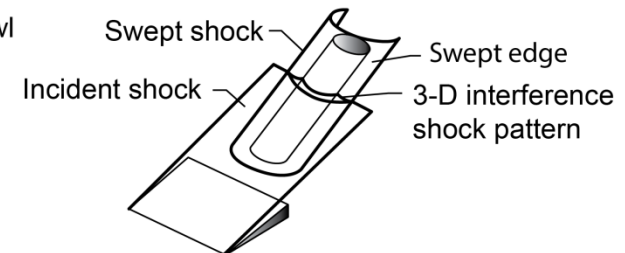
3D shock-on-fin (strut) cases were investigated in this study

Experimental simulation

Cowl



Struts

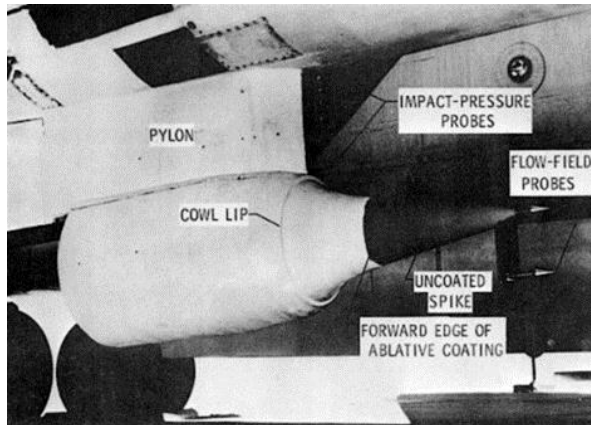




Historical Perspective



X-15 damage during Mach 6.7 hypersonic flight (October 1967)



<http://www.hq.nasa.gov/office/pao/History/x15lect/structur.html>



Damaged dummy ramjet

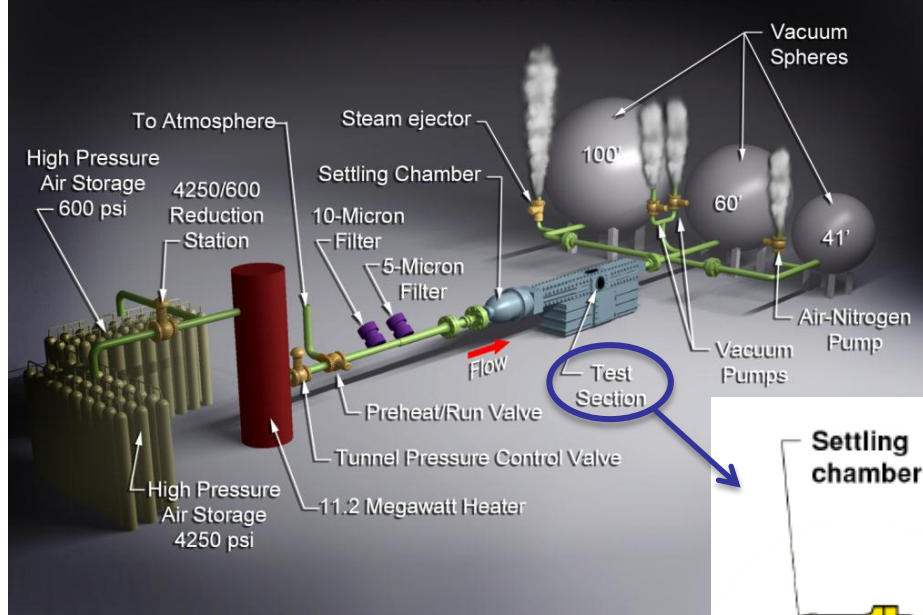


Damaged pylon



Conventional blow-down tunnel with rectangular cross-section

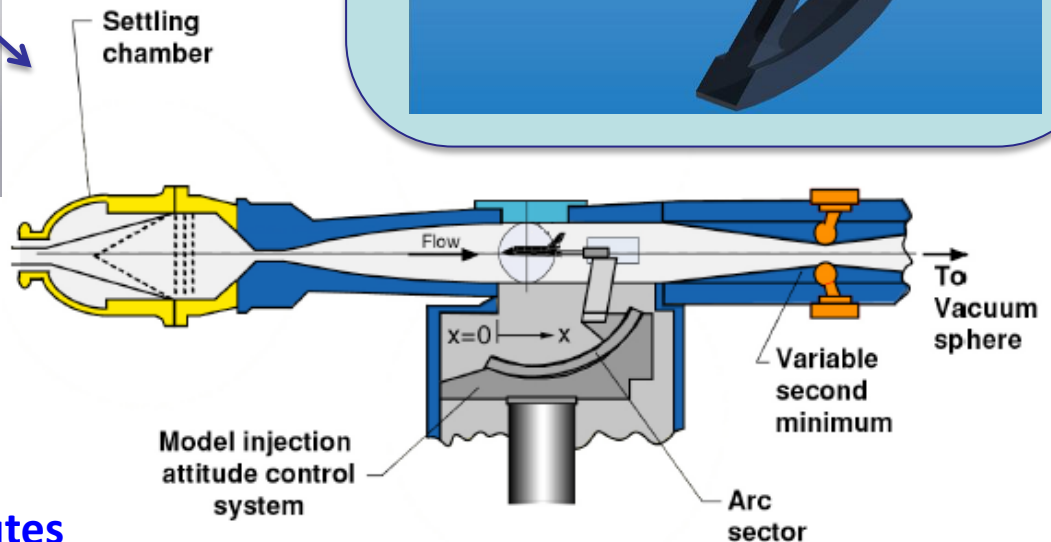
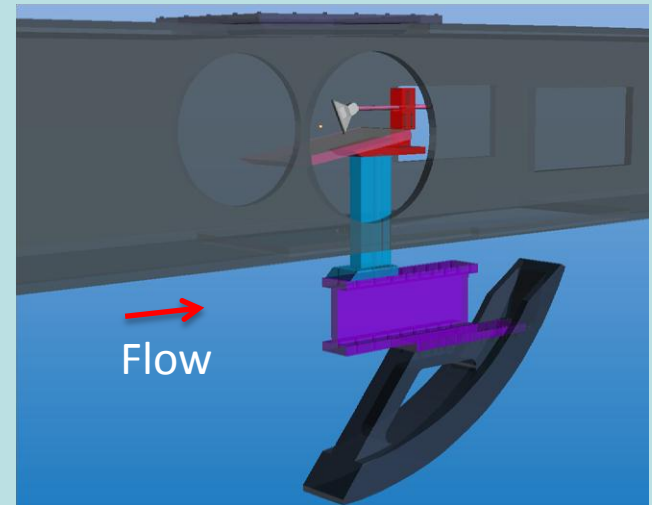
LAL 20-Inch Mach 6 Air Tunnel



Nominal Tunnel Conditions:

- Mach 6, Re: $0.5-8.0 \times 10^6/\text{ft}$
- $T_{t,1}$: 410-475° F
- $P_{t,1}$: 30-475 psia
- Test section: 20.5" x 20.0"
- Run duration: Up to a few minutes

Graphic rendering of the present model in the test section:





Experimental Approach



- Design and build test articles with cylindrical leading edges
- Utilize the 20-Inch Mach 6 Air Tunnel to simulate shock-shock interactions expected in hypersonic flight
- Analyze the flow patterns above (schlieren) and at (oil flow) the test article surface
- Develop 1D semi-infinite code based on a legacy program to analyze the heat transfer to the test article
- Develop 1D and 2D finite-volume codes to analyze the heat transfer to the test article

Test 6976	– Exploratory study to test custom zoom schlieren system	March 2012
Test 6983 Phase 1	– Conducted oil-flow visualization test with metal models and obtained high-speed zoom schlieren data	August 2012
Test 6983 Phase 2	– Performed phosphor thermography tests with fused silica models, and improved high-speed zoom schlieren	October 2012

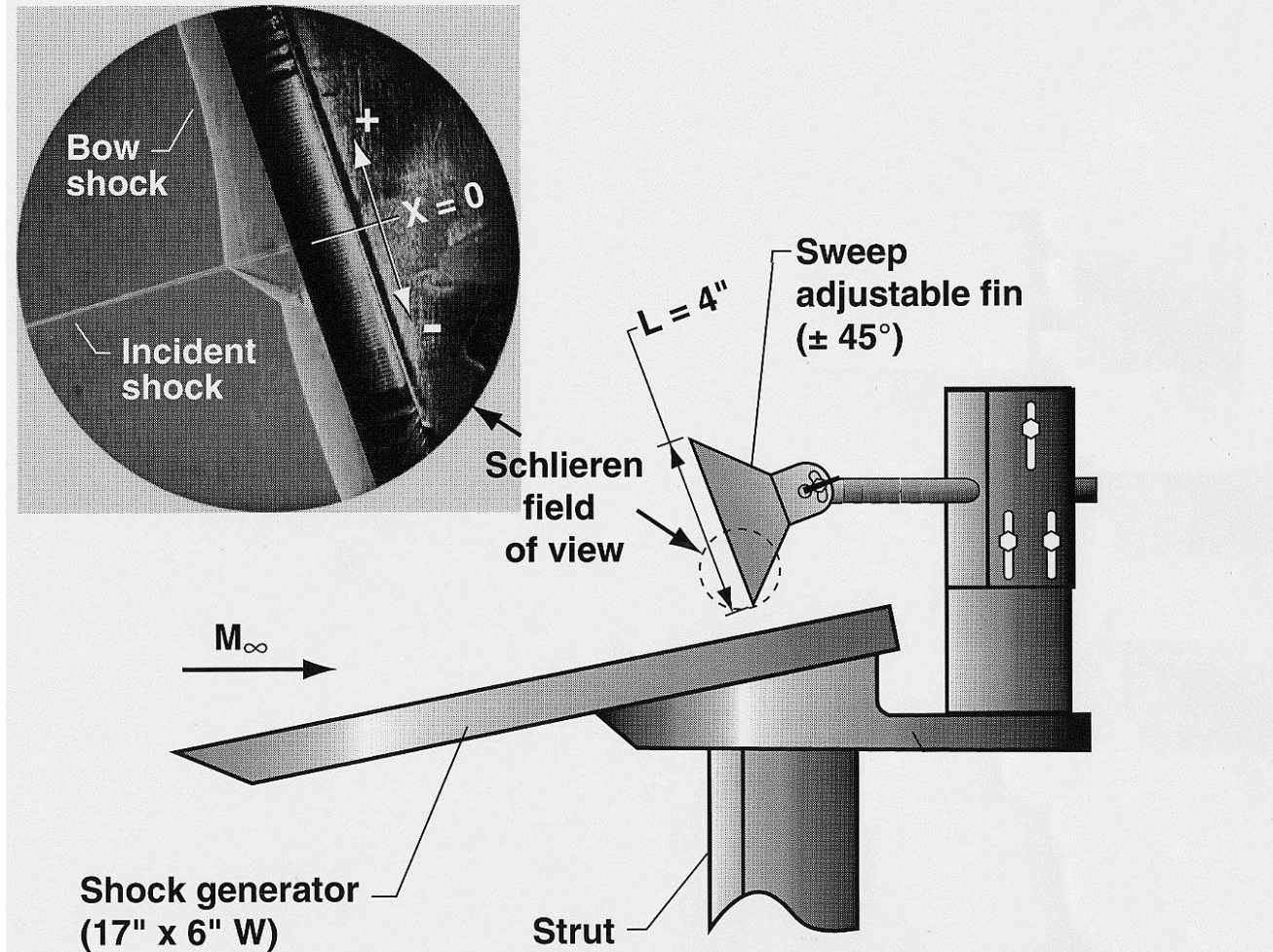


Test Set-up



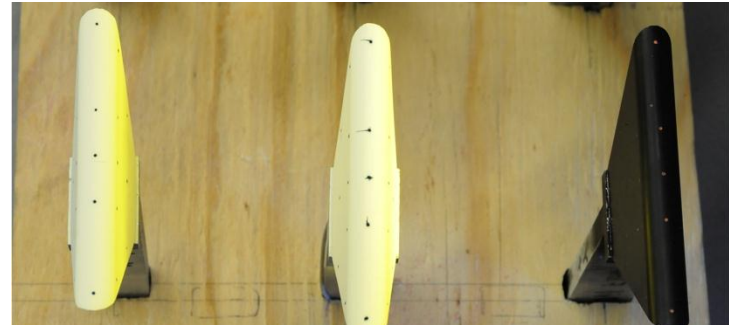
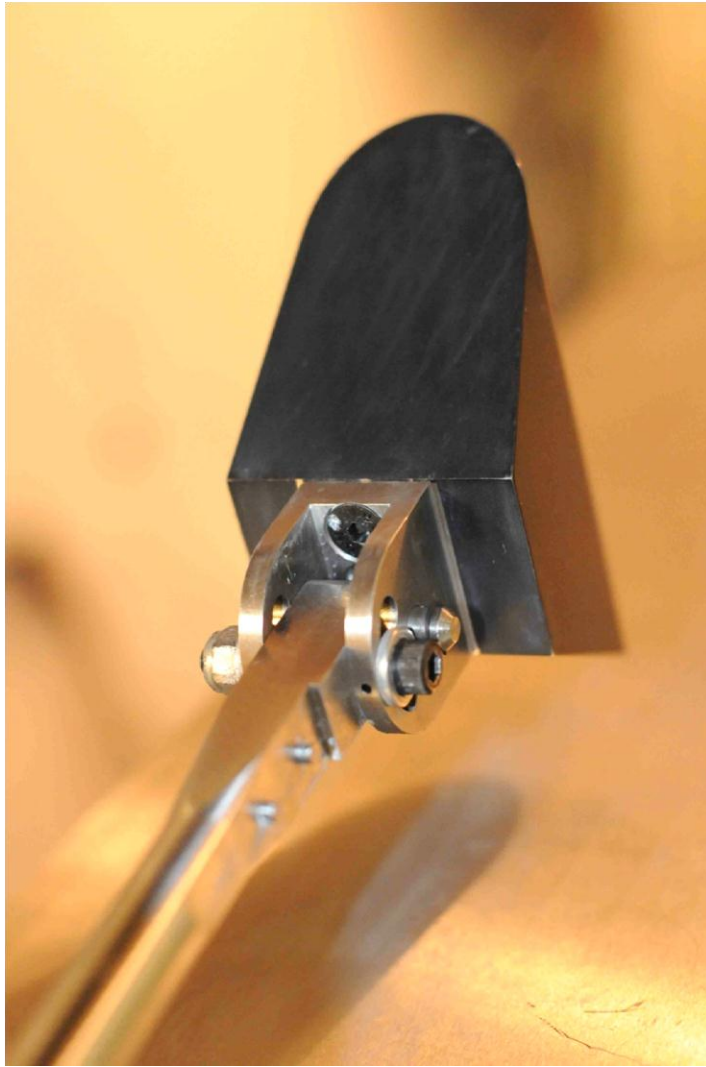
Previous shock-on-strut experiment (see Berry & Nowak, 1997):

Experimental Set-up





Test Set-up



$r_{\text{nose}} = 0.25$ inches



$r_{\text{nose}} = 0.50$ inches



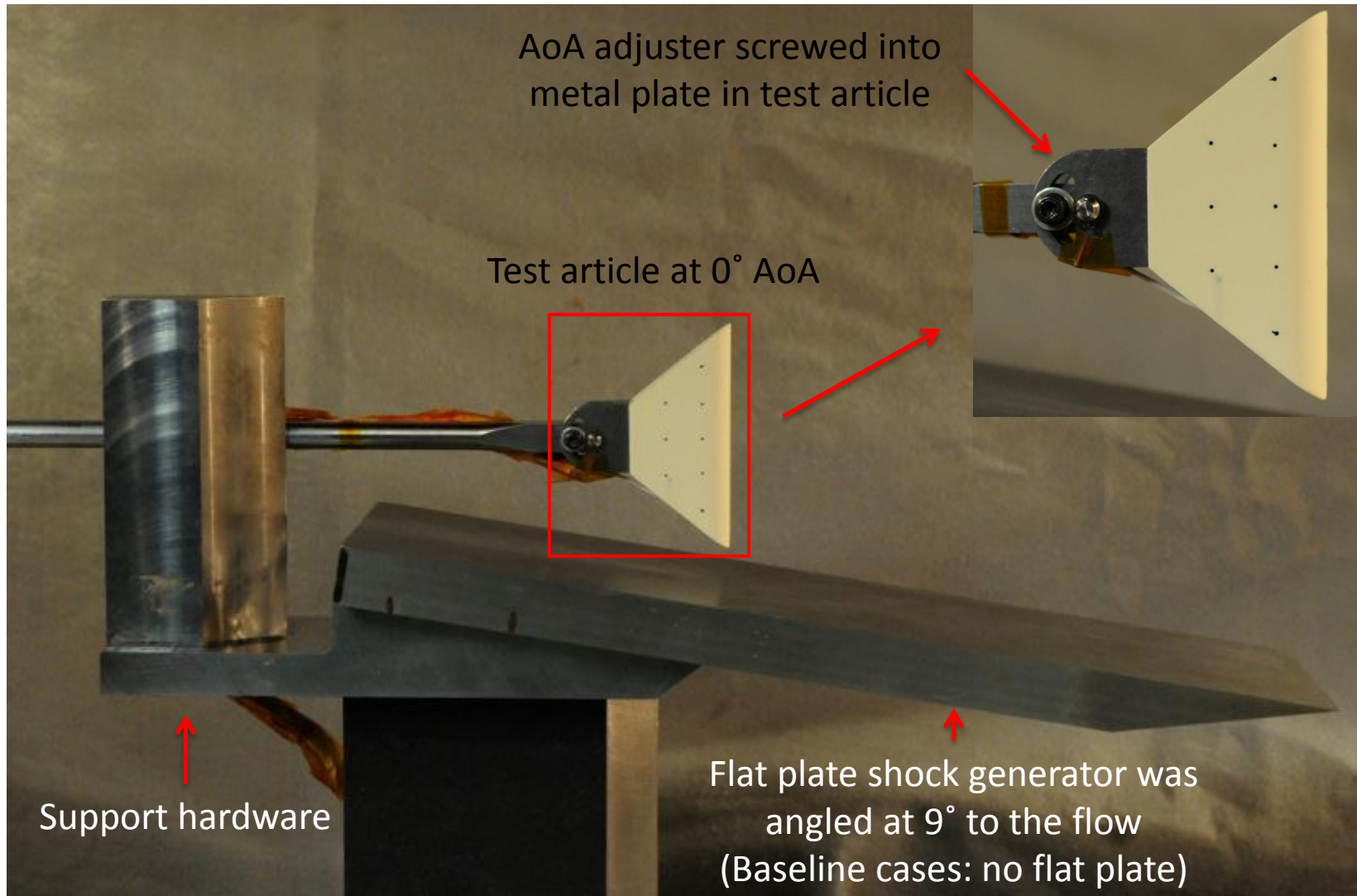
$r_{\text{nose}} = 0.75$ inches

Fused Silica

Metal



Test Set-up

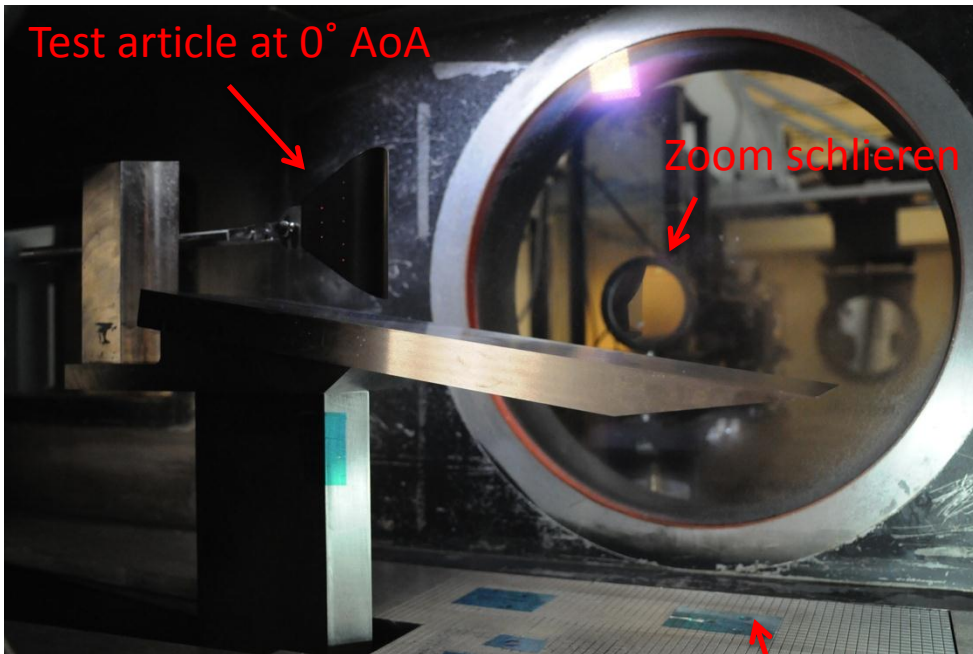




Test Set-up



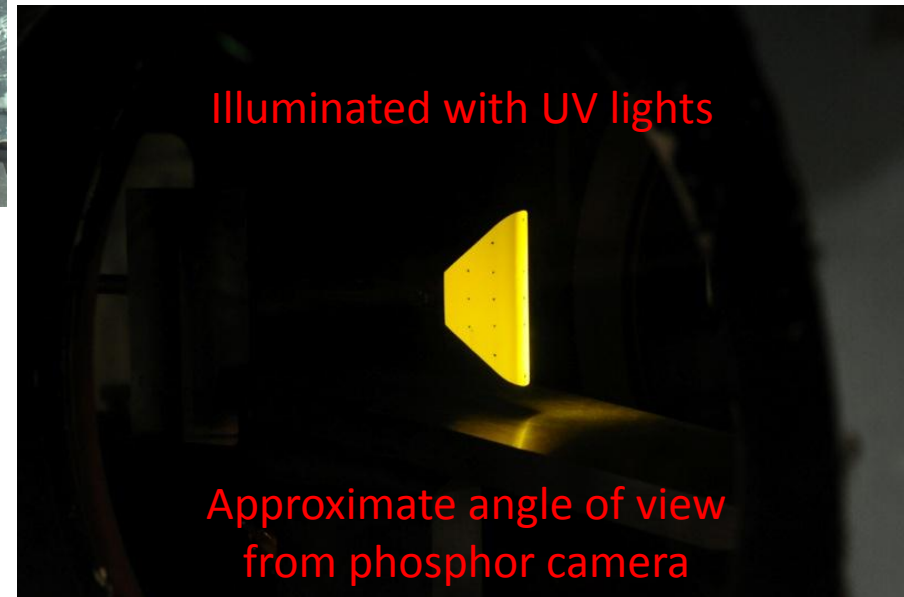
Test 6983: Oil Flow



Tunnel floor plate

Test articles were inserted into the tunnel test section in about 1.5s and each run lasted 3-10 seconds

Test 6983: Phosphor Thermography





Test Matrix



Test Article and Support Hardware Configurations for Test 6976 and Test 6983

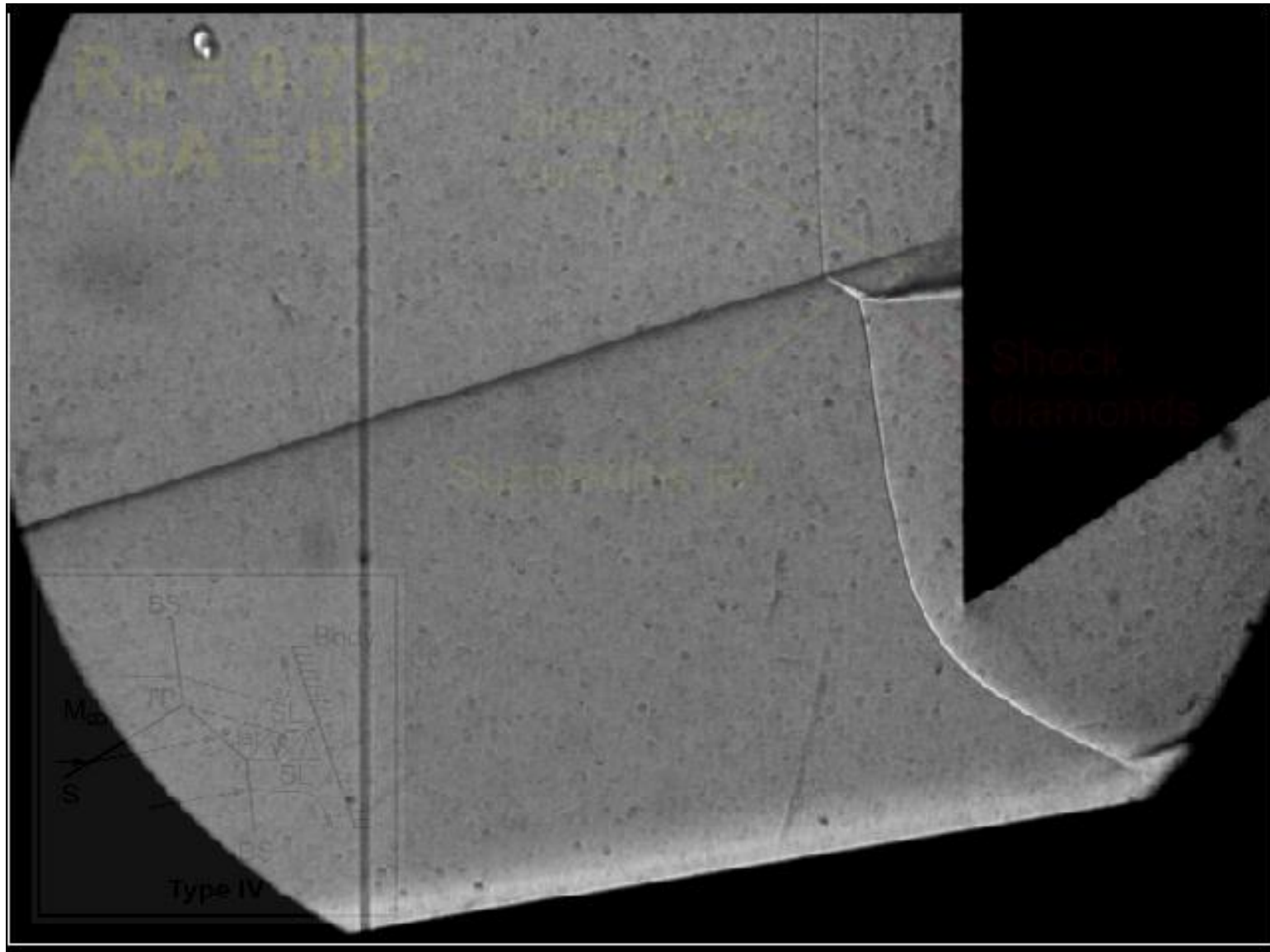
Test	Test Article			S.G. Angle	Type of Data Acquired		Re #, ft ⁻¹ x10 ⁻⁶
	Type	Nose Diameter	AoA		Schlieren	Other	
6976	Macor®, Upilex®	0.5"	0°	6°, 9°	30 fps	Thin film	2.1
6983-1	Metal	0.5", 1.0", 1.5"	-15°	9°	1000-1600 fps	Oil flow	2.1
6983-2	Fused Silica	0.5", 1.0", 1.5"	-25°	9°	7900-28000 fps	Phosphor	1.1, 2.1, 4.1

Averaged Flow Conditions for 20-Inch Mach 6 Air Tunnel

Test	M _∞	P _{t,1} , psia	T _{t,1} , °R	Re _∞ , ft ⁻¹ x10 ⁻⁶	ρ _∞ , 10 ⁻⁴ slug/ft ³	T _∞ , °R	V _∞ , ft/s
6983	5.90	60.5	875.1	1.1	0.33	110.3	3035
6976	5.96	126.4	894.7	2.1	0.64	110.7	3073
6983	5.96	125.5	898.5	2.1	0.63	111.3	3082
	6.00	252.2	901.6	4.1	1.23	110.5	3087

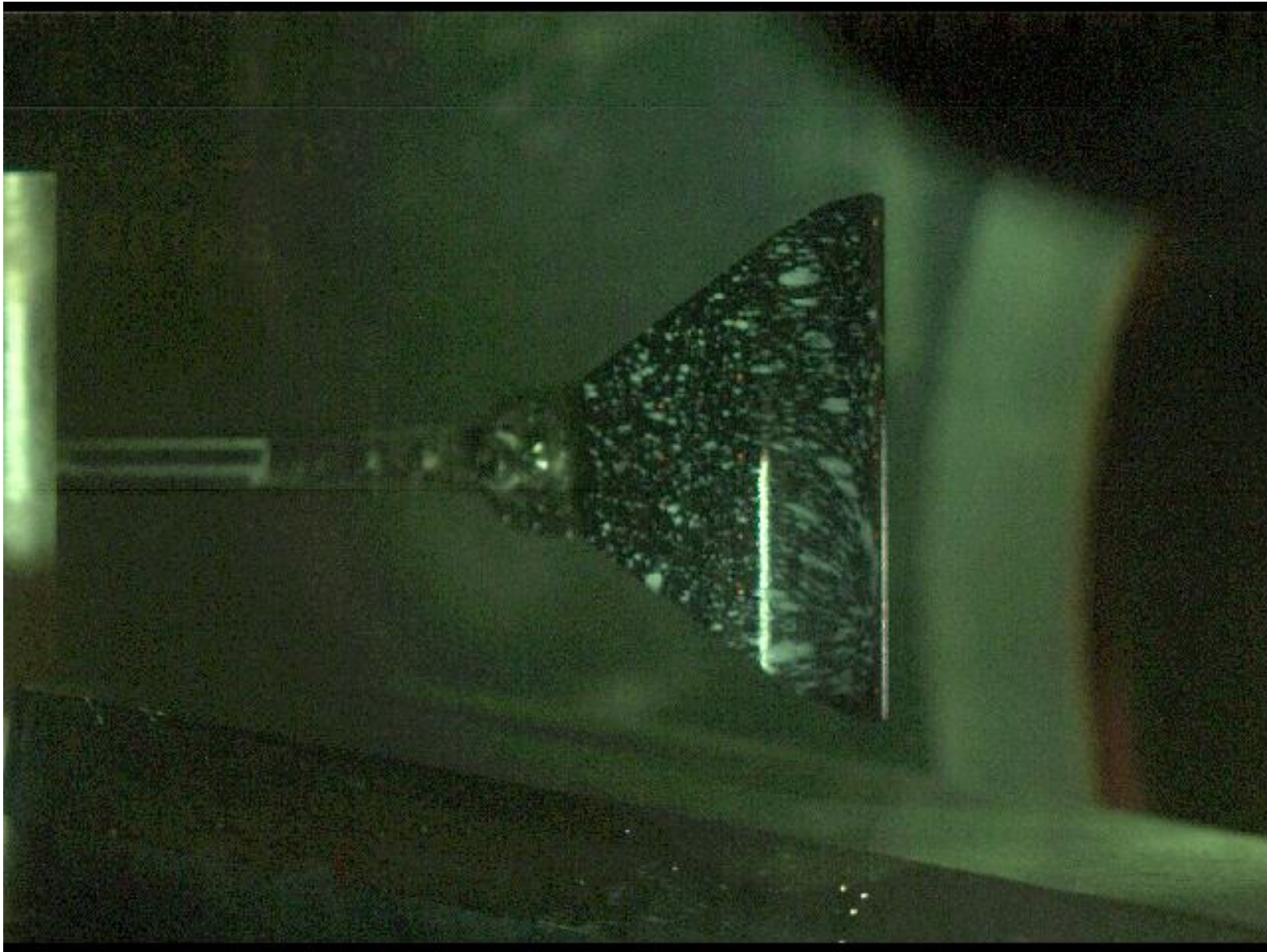


Experimental Zoom Schlieren



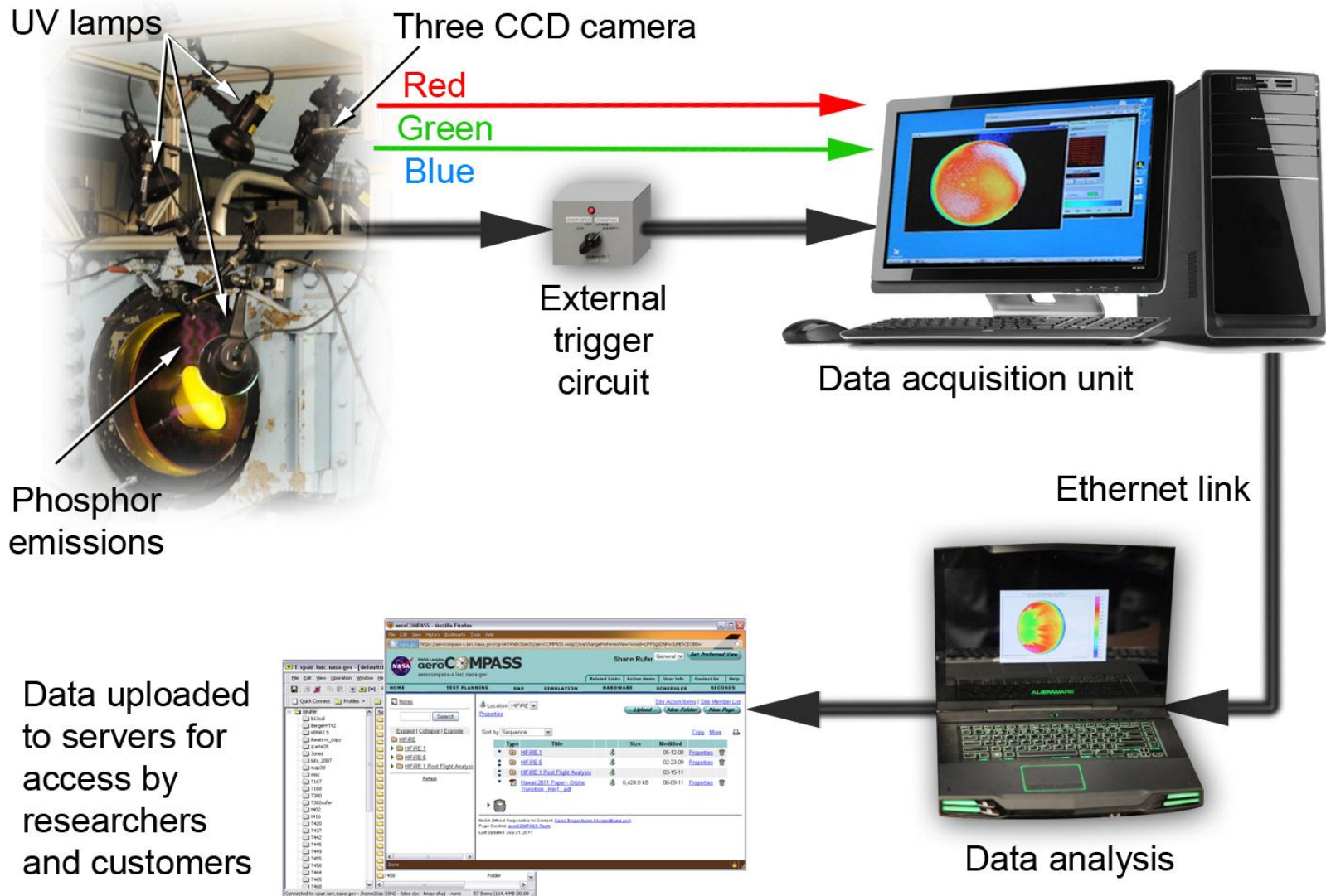


Oil Flow Tests



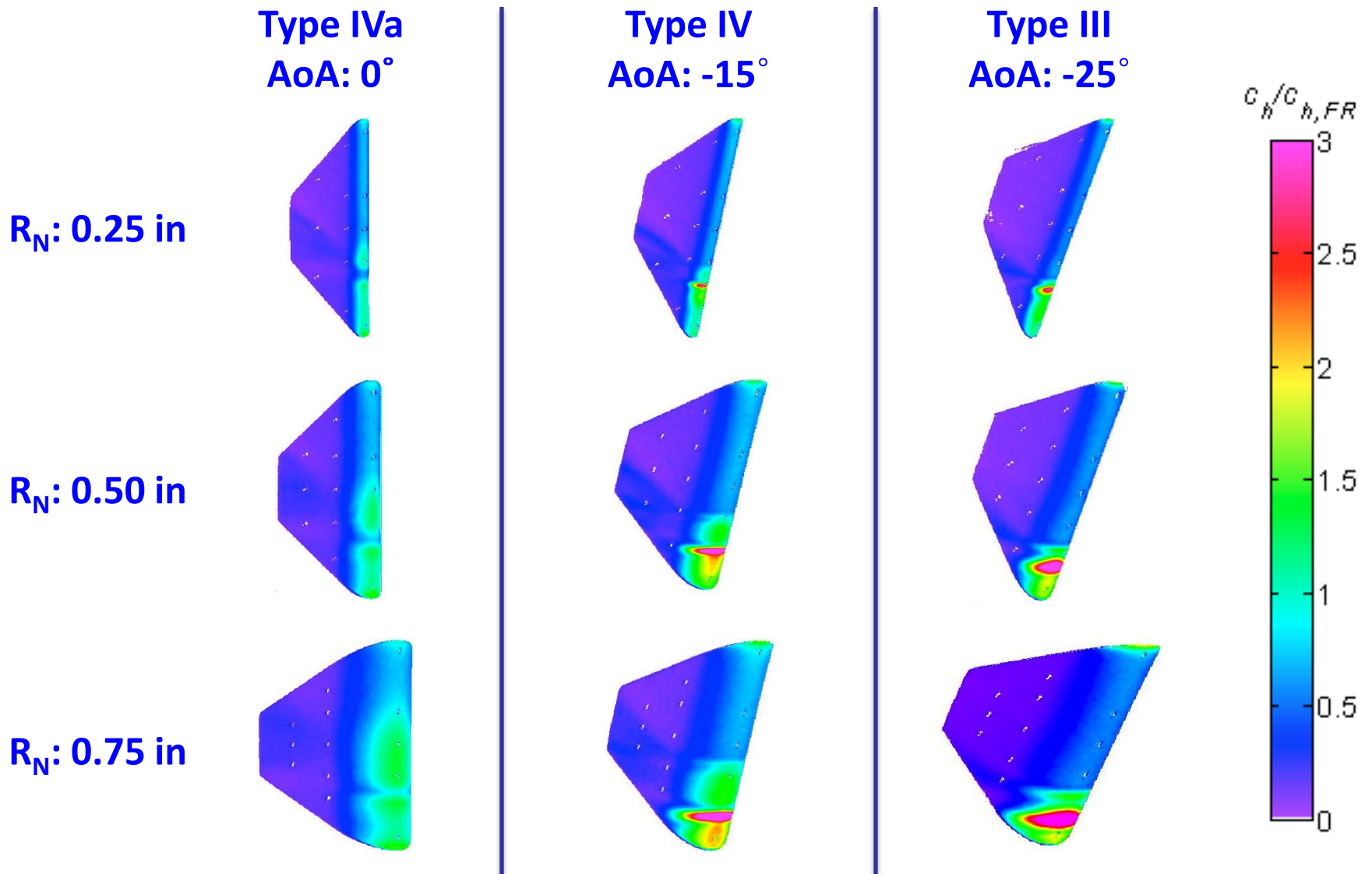


Phosphor Thermography





1D Global Heating Contour Maps



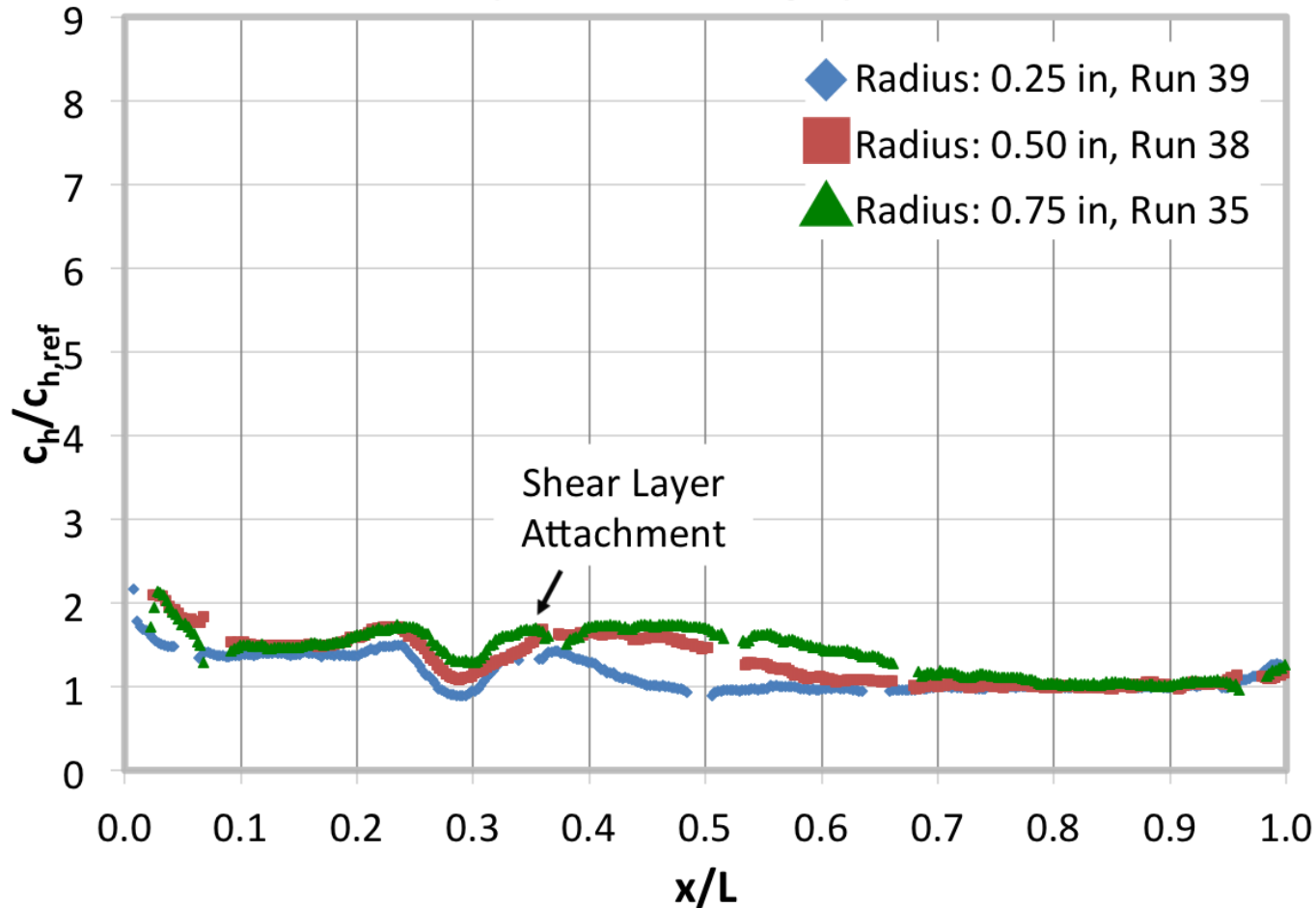


Heat Transfer Data

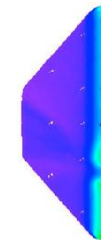


Non-dimensional Heat Transfer Coefficients

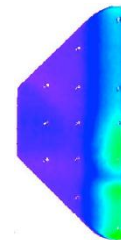
AoA = 0°, Re = 2.1×10^6 /ft, $t = 1.8$ s



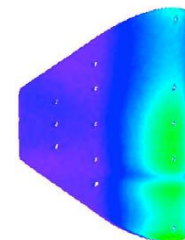
Type IVa
AoA: 0°



Run 39



Run 38



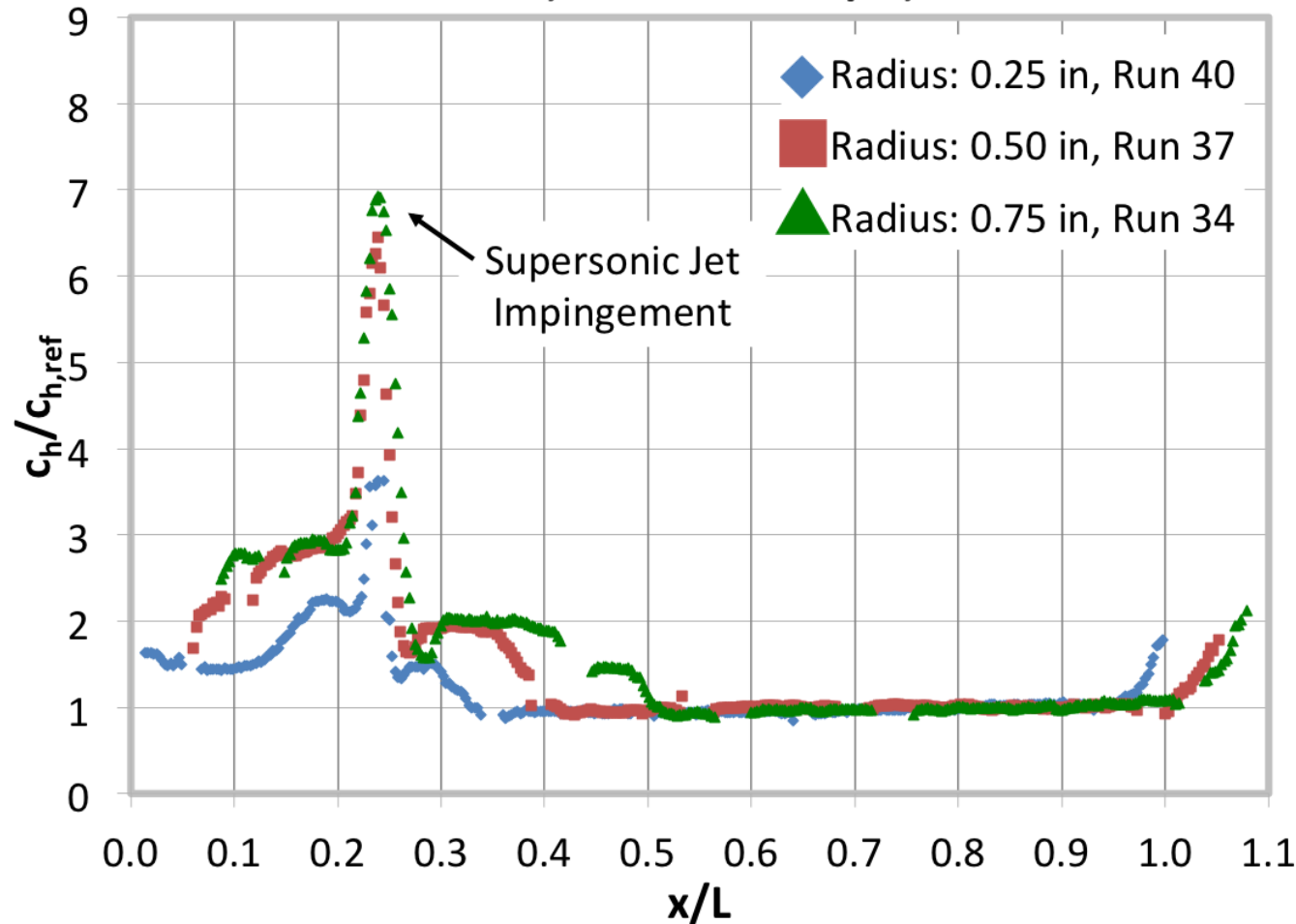
Run 35



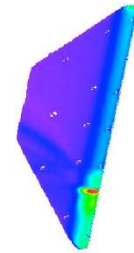
Heat Transfer Data



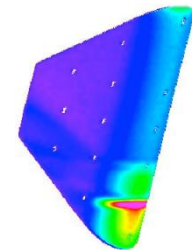
Non-dimensional Heat Transfer Coefficients
AoA = -15° , $Re = 2.1 \times 10^6/ft$, $t = 1.8$ s



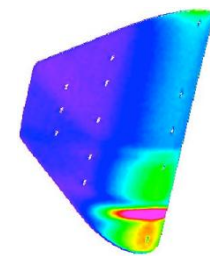
Type IV
AoA: -15°



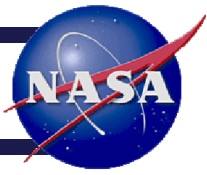
Run 40



Run 37



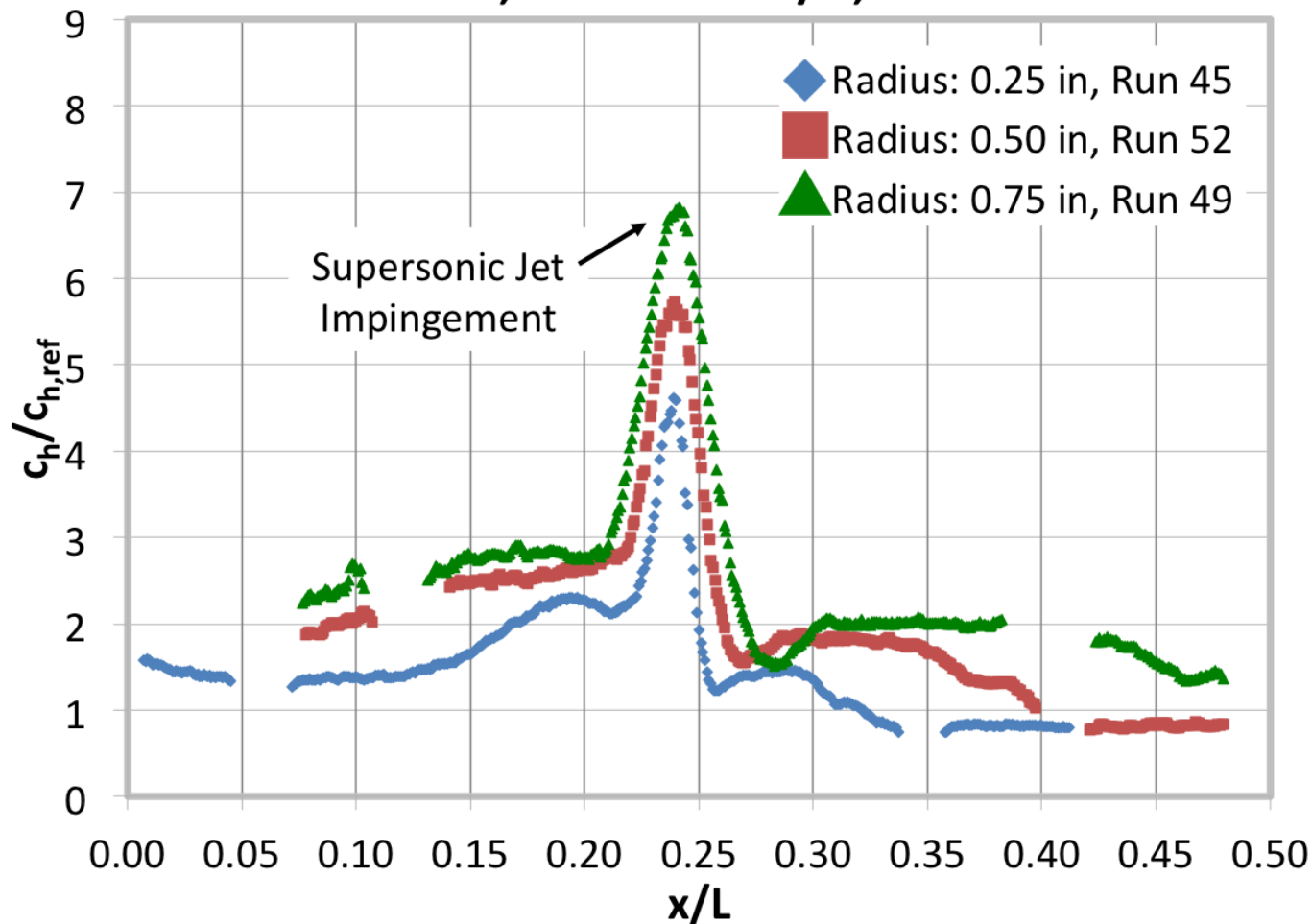
Run 34



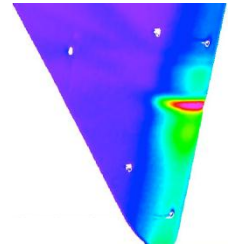
Heat Transfer Data

Non-dimensional Heat Transfer Coefficients

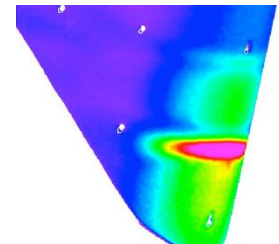
AoA = -15° , $Re = 2.1 \times 10^6/ft$, $t = 1.8$ s



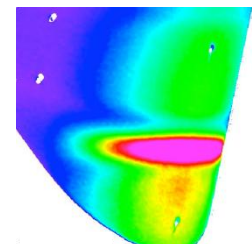
Type IV
AoA: -15°



Run 45



Run 52



Run 49

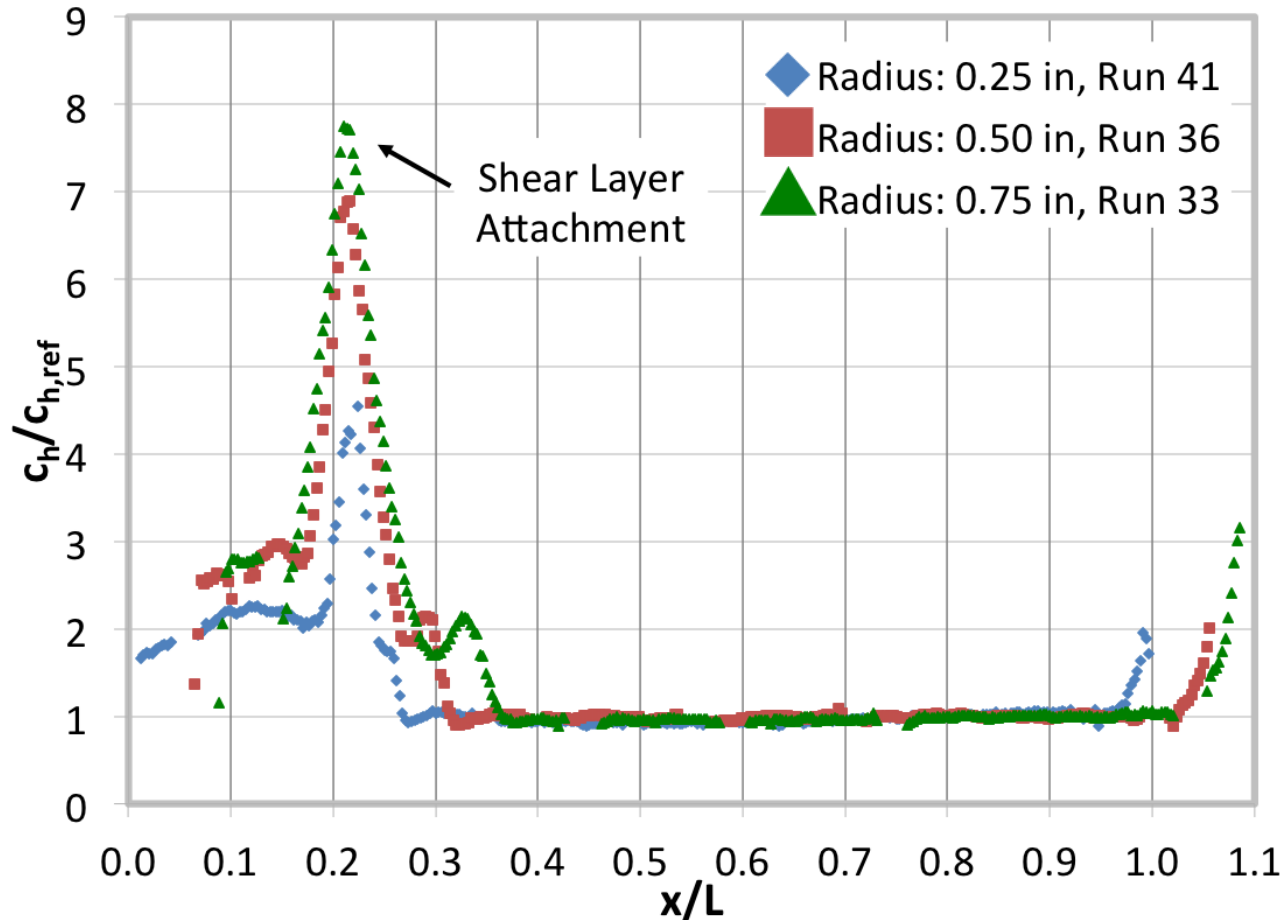


Heat Transfer Data

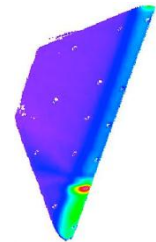


Non-dimensional Heat Transfer Coefficients

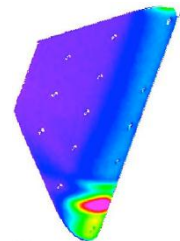
AoA = -25° , $Re = 2.1 \times 10^6/ft$, $t = 1.8$ s



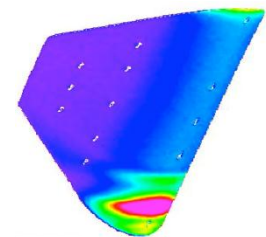
Type III
AoA: -25°



Run 41



Run 36



Run 33

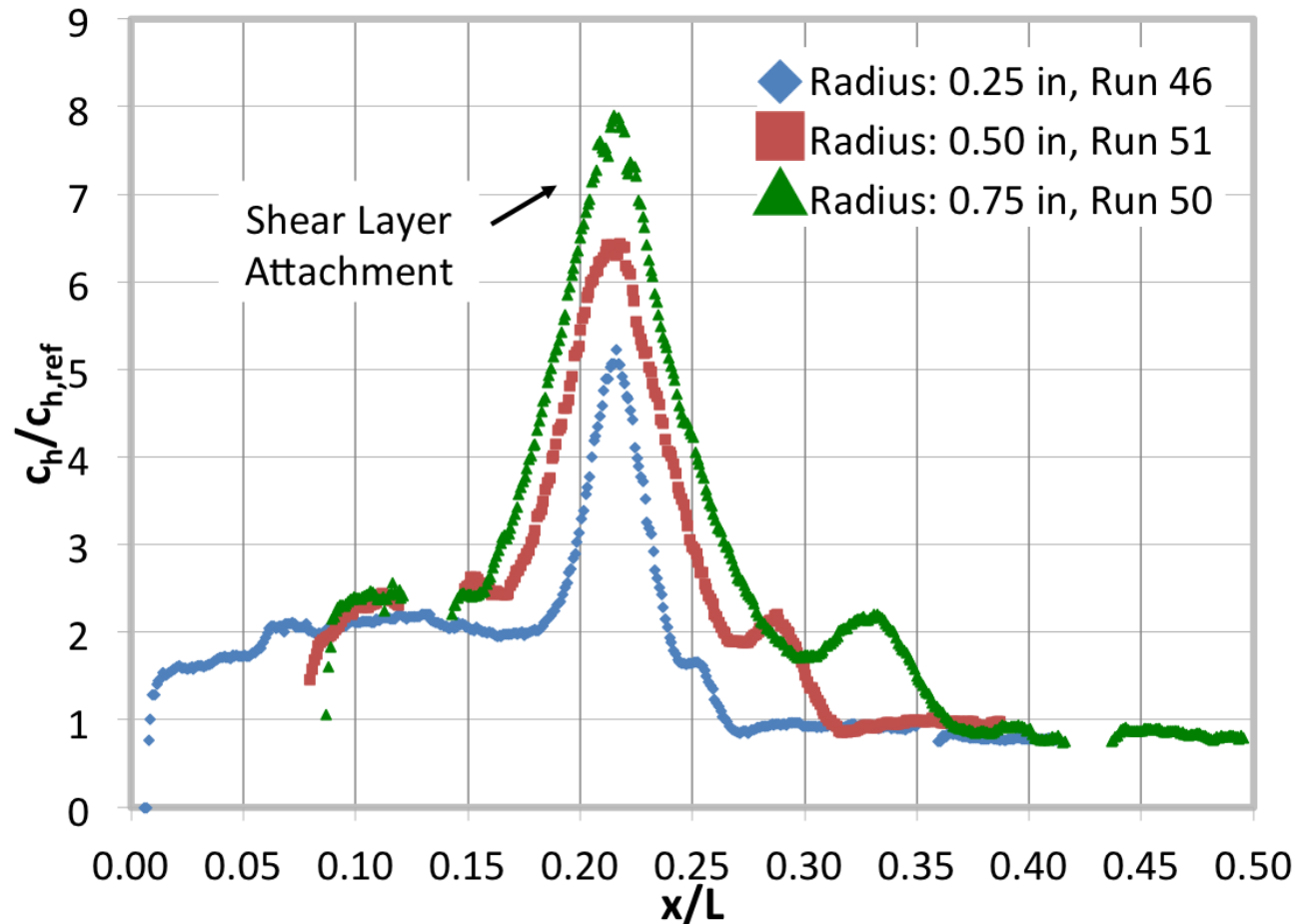


Heat Transfer Data

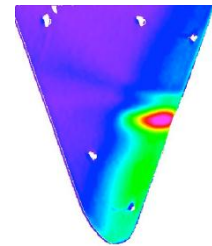


Non-dimensional Heat Transfer Coefficients

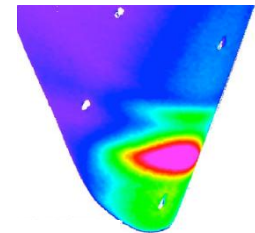
AoA = -25° , $Re = 2.1 \times 10^6/ft$, $t = 1.8$ s



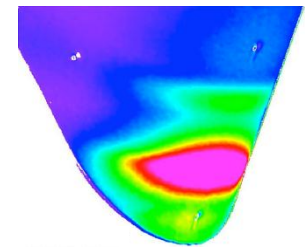
Type III
AoA: -25°



Run 46



Run 51



Run 50

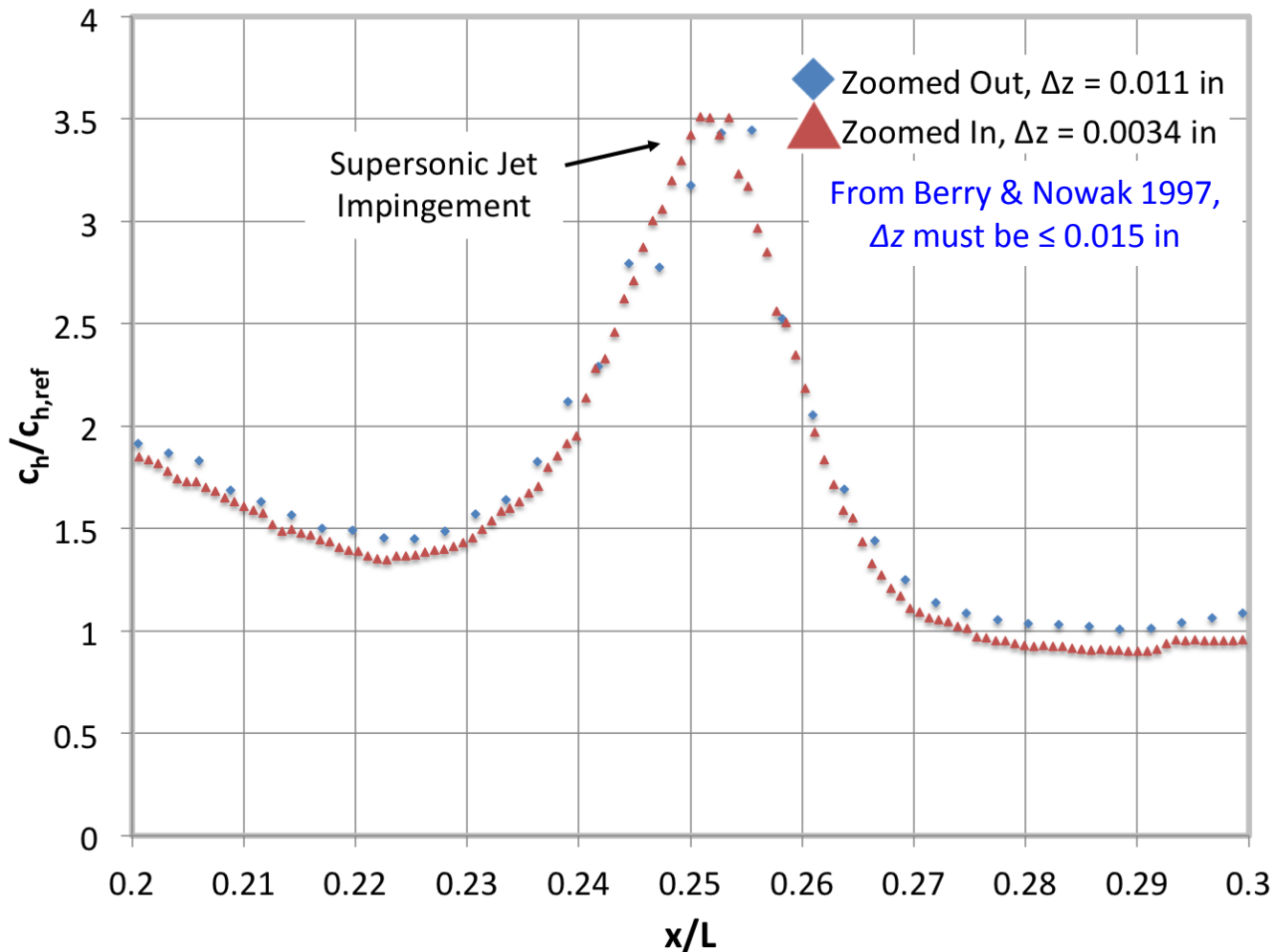


Spatial Resolution

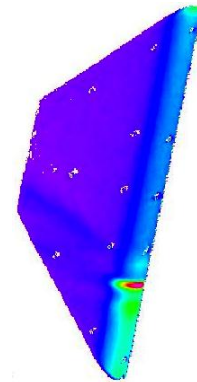


IHEAT Non-dimensional Heat Transfer Coefficients

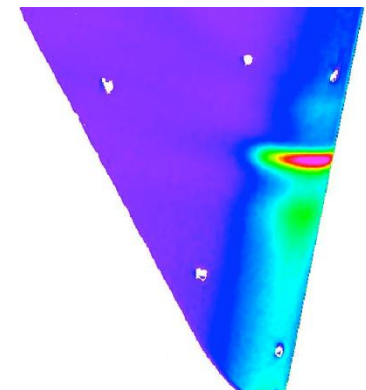
R_N : 0.25 in, $t = 4.6$ s, Re : $1.1 \times 10^6/ft$, AoA : -15°



Type IV
 AoA : -15°



Run 43



Run 44



1D IHEAT Code:

- Semi-infinite conduction
- Convection boundary condition (BC)

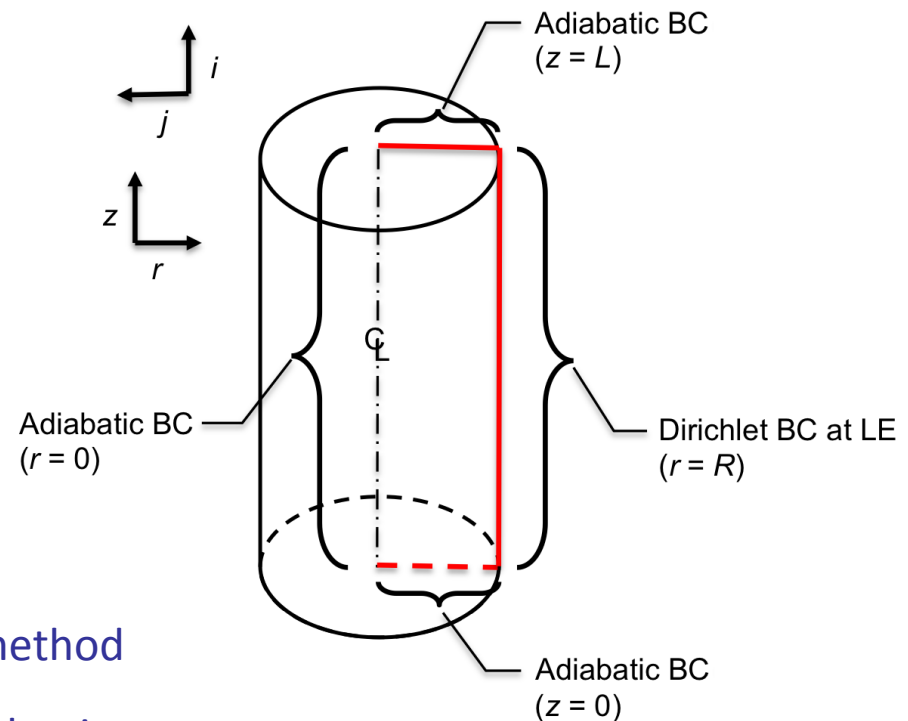
1D Finite-Volume Code:

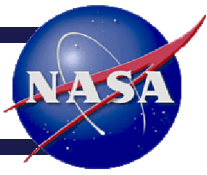
- Direct Crank-Nicolson method
- Neglects curvature, radial conduction only
- Unconditionally stable, grid converged

2D Finite-Volume Code:

- Direct Alternating Direction Implicit (ADI) method
- Cylindrical geometry, radial and lateral conduction
- Unconditionally stable, grid converged

Boundary conditions for finite-volume codes

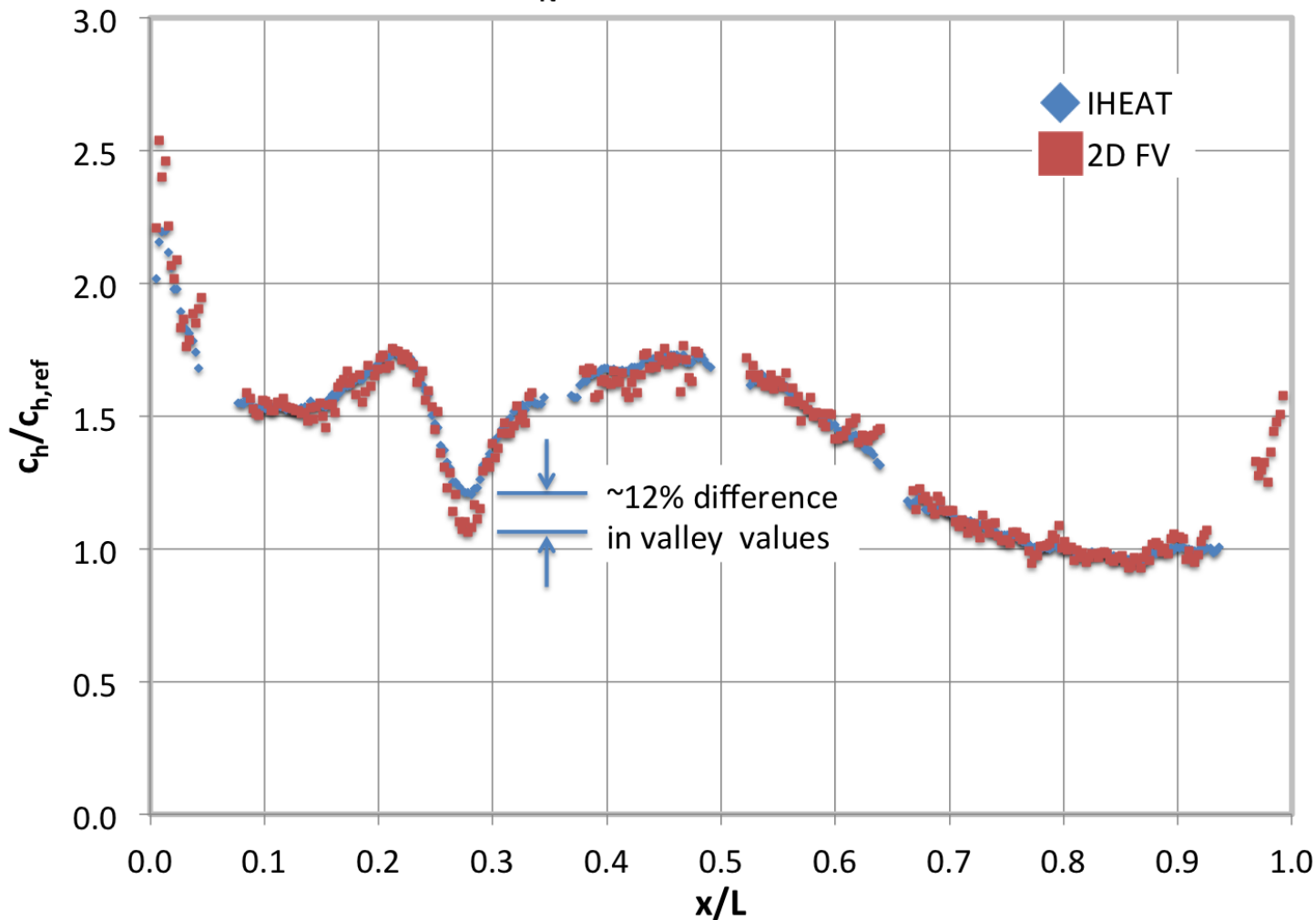




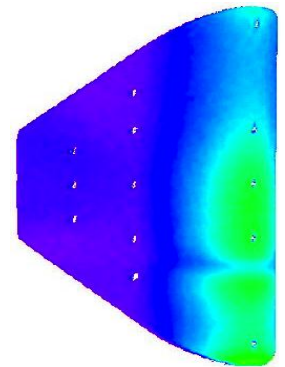
1D versus 2D Heat Transfer

Non-dimensional Heat Transfer Coefficients, 1D versus 2D

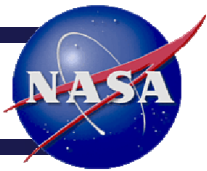
Run 35, $t = 4.6$ s, $R_N: 0.75$ in, $Re: 2.1 \times 10^6/ft$, $AoA: 0^\circ$



Type IVa
 $AoA: 0^\circ$



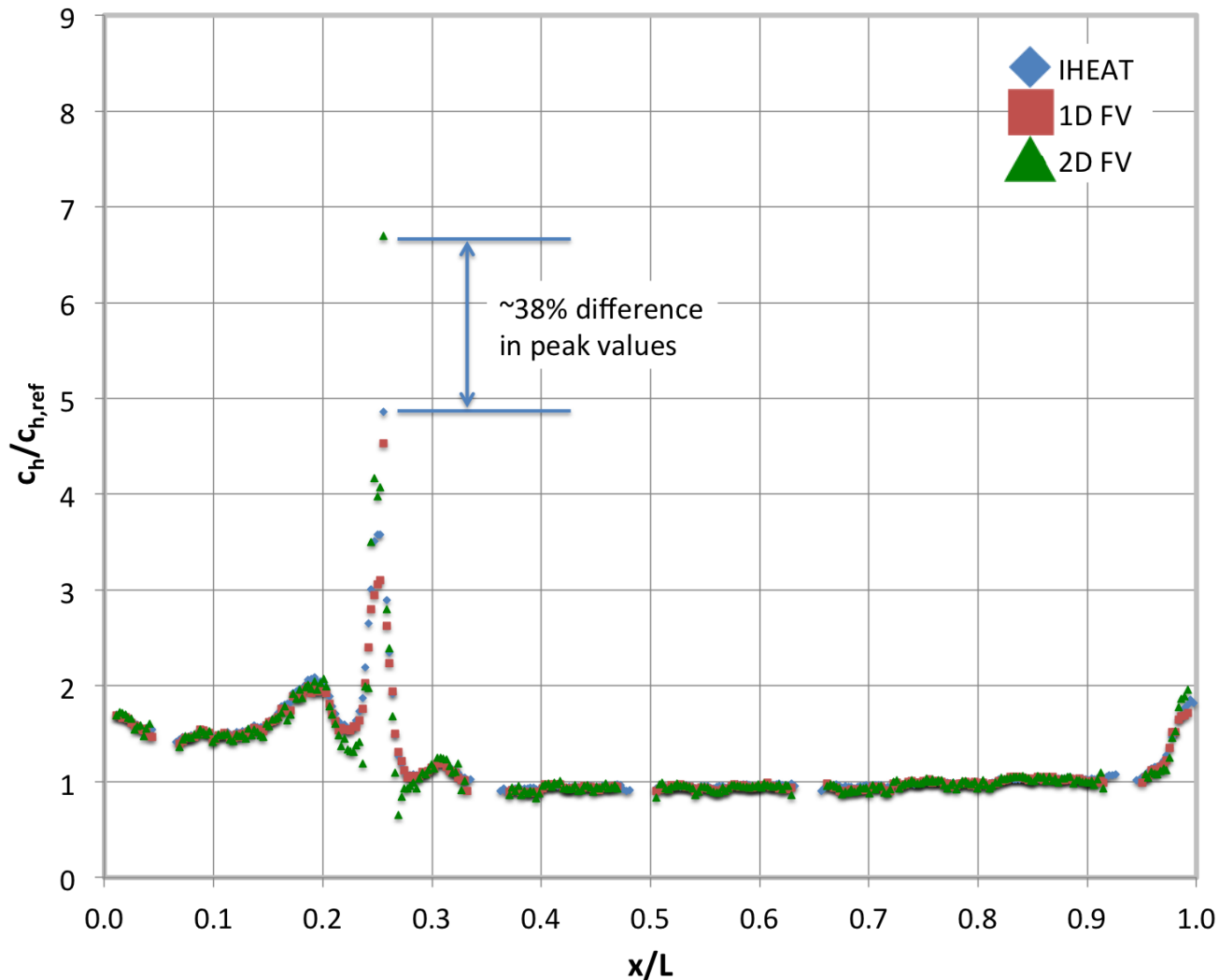
Run 35



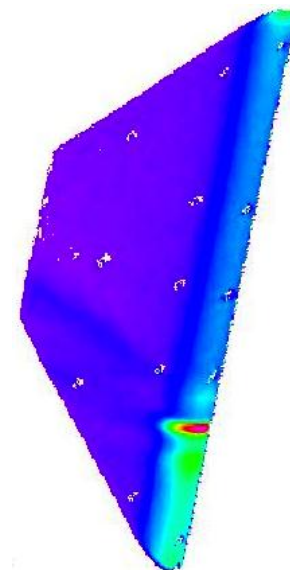
1D versus 2D Heat Transfer

Non-dimensional Heat Transfer Coefficients, 1D versus 2D

Run 43, $t = 3.4$ s, $R_N: 0.25$ in, $Re: 1.1 \times 10^6/ft$, $AoA: -15^\circ$



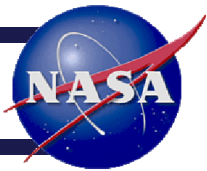
Type IV
 $AoA: -15^\circ$



Run 43

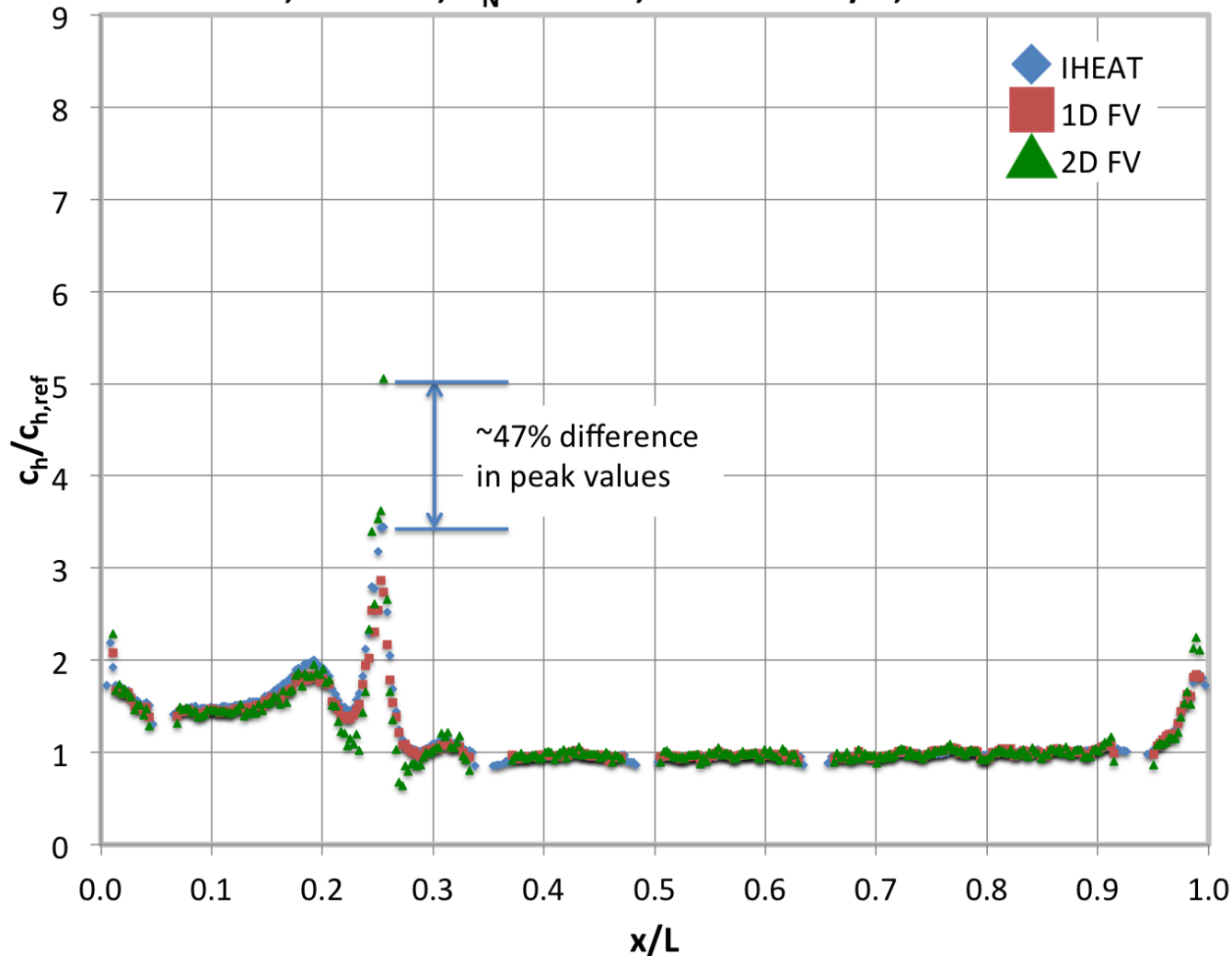


1D versus 2D Heat Transfer

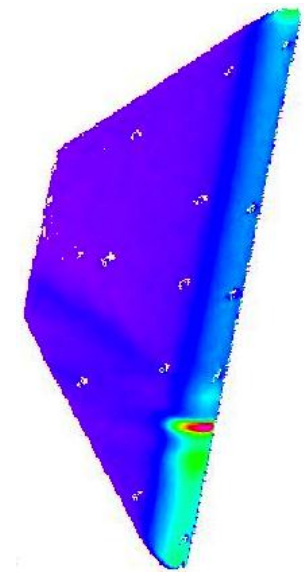


Non-dimensional Heat Transfer Coefficients, 1D versus 2D

Run 43, $t = 4.6$ s, R_N : 0.25 in, Re : 1.1×10^6 /ft, AoA : -15°



Type IV
 AoA : -15°



Run 43

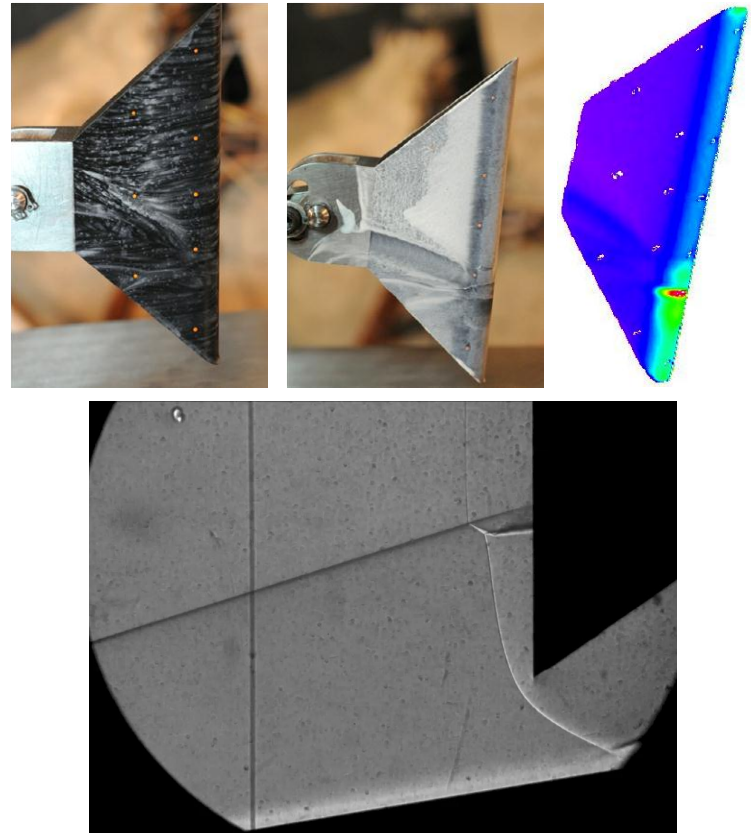


Conclusions

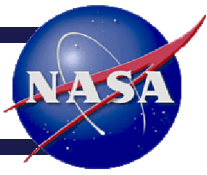


- Of the cases considered, the smallest leading-edge radius produced the worst case dimensional peak heat transfer augmentation
 - Type III interaction for $\text{AoA} = -25^\circ$
 - Type IV interaction for $\text{AoA} = -15^\circ$
- All the shock-shock interaction cases behave similarly for the three test article geometries
- Oil flow and zoom schlieren results show the main effects of shock-shock interactions are confined to specific regions on the test article
- Multi-dimensional heat transfer analyses that account for lateral conduction are required if sharp temperature gradients exist
- A spatial resolution of 0.015 in is sufficient to capture the peak heat transfer due to a Type III or Type IV shock-shock interaction

First global thermal imaging study to improve the understanding of 3D shock-on-strut interactions



Thank you! Questions?



Back-up Slides



- Obtain global temperature data later in wind tunnel runs with similar test articles and either
 - A higher temperature phosphor system
 - An IR system (with at least 640x480 resolution)
- Improve the 2D FV code
 - Include additional geometries
 - Finish debugging the Douglas-Gunn method
- Develop a 3D Douglas-Gunn FV code to use in IHEAT
 - Implement a 3D mapping algorithm to correlate the temperature data in the 2D image to the 3D CAD geometry of the test article
 - Test the 3D code using the shock-shock interaction data to compare to the 1D and 2D results



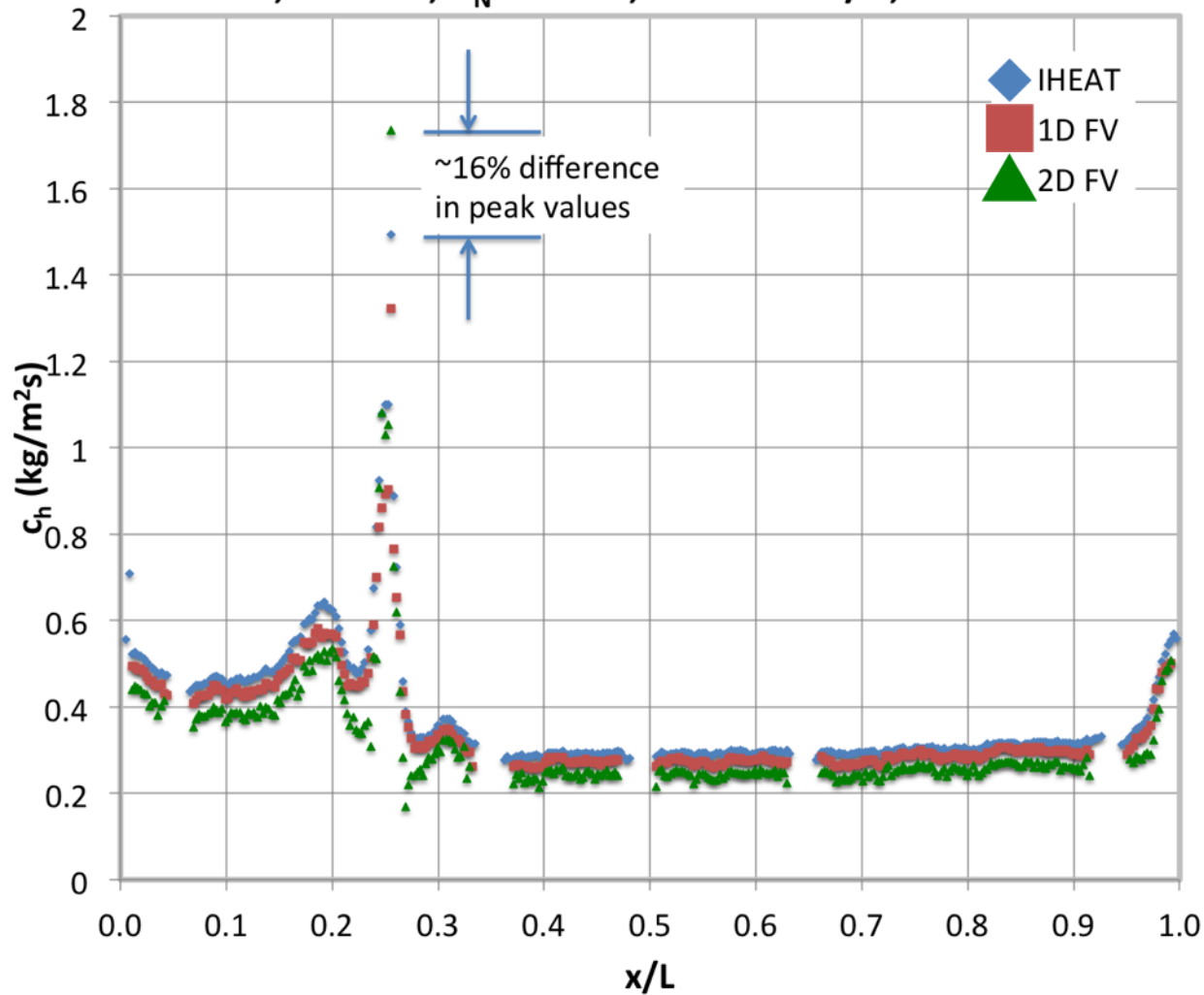
- If higher temperature data can be obtained, consider the following additional cases
 - Higher Reynolds numbers ($4 \times 10^6/\text{ft}$, $8 \times 10^6/\text{ft}$) using high-speed zoom schlieren to capture the unsteady flow features
 - Consider the effects of using a 12° SG angle
 - Test at the 31-Inch Mach 10 tunnel where the test articles heat up even more quickly so a 2D analysis may be more critical
 - Move the fins down closer to the shock generator plate to investigate the effects of shock-BL interactions in addition to the characterized shock-shock interactions
- Compare the 1D and 2D results for a zoomed-in case, properly converting the results to non-dimensional data



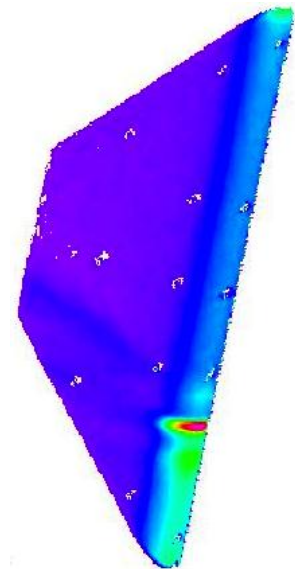
Heat Transfer Data



Dimensional Heat Transfer Coefficients, 1D versus 2D
Run 43, $t = 3.4$ s, $R_N: 0.25$ in, $Re: 1.1 \times 10^6/ft$, $AoA: -15^\circ$



Type IV



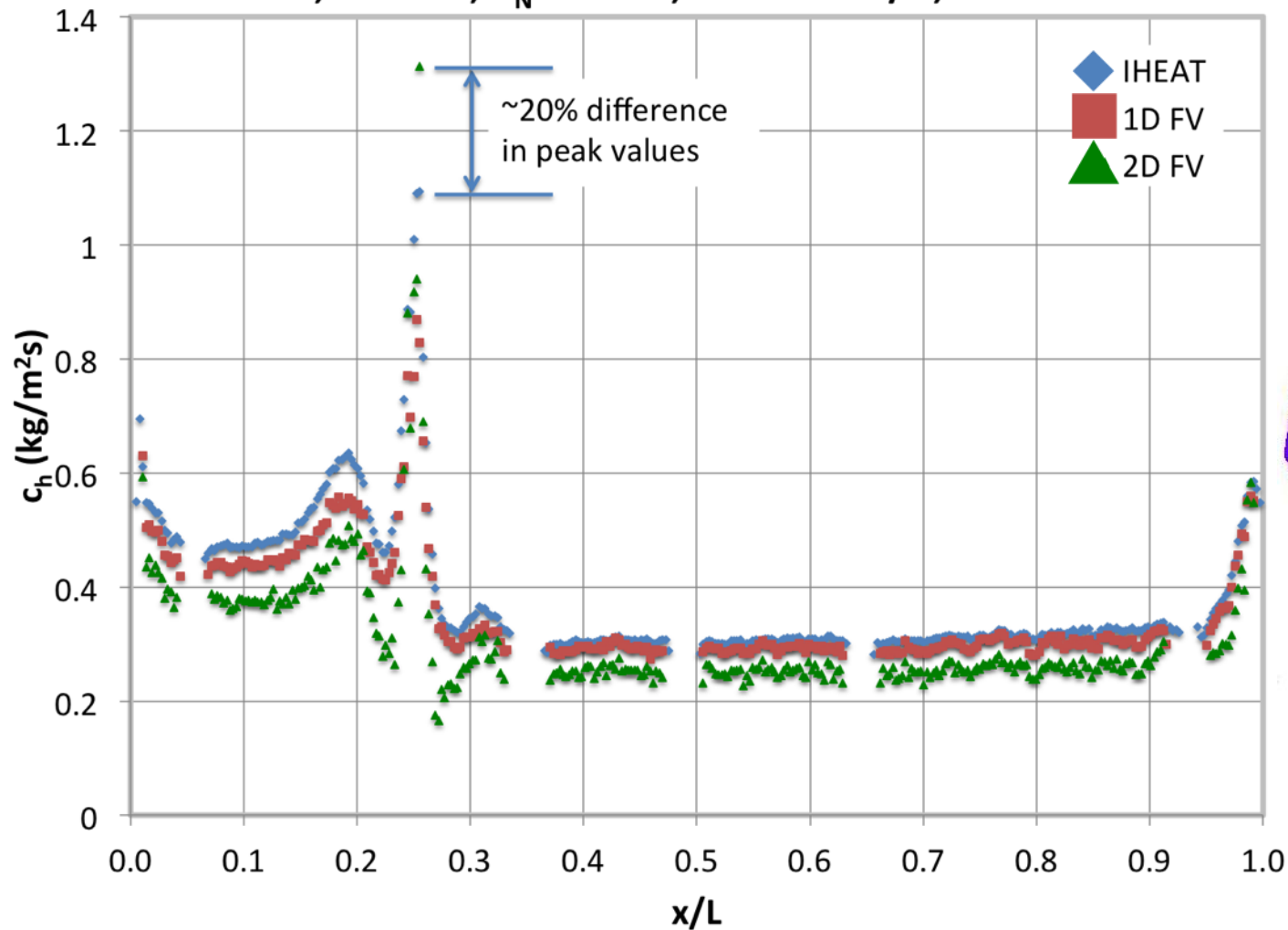
Run 43



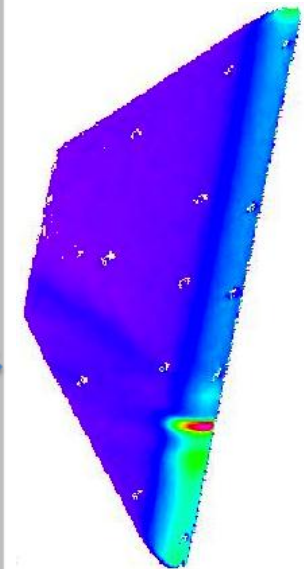
Heat Transfer Data



Dimensional Heat Transfer Coefficients, 1D versus 2D
Run 43, $t = 4.6$ s, $R_N: 0.25$ in, $Re: 1.1 \times 10^6/ft$, $AoA: -15^\circ$



Type IV



Run 43